

Measurement of number-phase uncertainty relations of optical fields

D. T. Smithey, M. Beck, J. Cooper,* and M. G. Raymer

Department of Physics and Chemical Physics Institute, University of Oregon, Eugene, Oregon 97403

(Received 20 April 1993)

We have experimentally determined all of the quantities involved in the uncertainty relation for the phase and photon number of a mode of the electromagnetic field when the field mode is in a coherent state of small average photon number. This is accomplished by determining the quantum state of the field using optical homodyne tomography, which uses measured distributions of electric-field quadrature amplitude to determine the Wigner function and hence the density matrix. The measured state is then used to calculate the uncertainty product for the number and phase, as well as the expectation value of the commutator of the number and phase operators. The experimental results agree with the quantum-mechanical predictions. We also present measured phase- and photon-number distributions for these weak coherent states, as well as their measured complex wave functions.

PACS number(s): 42.50.Wm, 03.65.Bz

I. INTRODUCTION

The uncertainty principle applied to electromagnetic fields implies that the field phase ϕ and photon number n cannot simultaneously have arbitrarily narrow distributions. Mathematically the uncertainty relation can be written as [1]

$$\Delta\phi\Delta n \geq \frac{1}{2} |\langle \Psi | [\hat{\phi}, \hat{n}] | \Psi \rangle|, \quad (1)$$

where the phase variance $\Delta\phi^2 = \langle \Delta\hat{\phi}^2 \rangle = \langle \hat{\phi}^2 \rangle - \langle \hat{\phi} \rangle^2$, Δn^2 is defined similarly, and the expectation values are taken over the state of the system $|\Psi\rangle$. The commutator $[\hat{\phi}, \hat{n}]$ is an operator, and its expectation value is in general state dependent. Thus, to set the lower bound of experimental measurements of $\Delta\phi\Delta n$, one needs a way to determine the expectation value on the right-hand side of Eq. (1) for the state of interest.

Here we describe an experiment which determines the variances of phase and photon number for an optical field containing small numbers of photons, as well as the expectation value of the number-phase commutator [2]. This is accomplished by experimentally measuring the quantum state of the field by using optical homodyne tomography (OHT) [3–5]. Since the determination of the quantities in Eq. (1) uses this measured state and assumes the validity of quantum mechanics, the experiment does not provide an independent verification of the uncertainty relation [i.e., a test that is independent of quantum-mechanical principles]. However, the measurements do allow one to determine, for an arbitrary state, how close the inequality of Eq. (1) comes to *equality*. For example, it is found for small-amplitude coherent states that equality in the uncertainty relation [Eq. (1)] is not achieved. States for which Eq. (1) is an equality have been called “intelligent states.” States which also minimize the right-hand side of Eq. (1) are called minimum-uncertainty states (MUS). As such, not all intelligent states are MUS [6]. Coherent states (other than the vacuum) are neither intelligent states, nor MUS, with respect to number and

phase.

For our measurements, the relevant interpretation of the uncertainty relation is that the state of the field does not have well-defined phase and photon number. Since neither the phase nor photon number of the field are measured on individual trials, the results do not directly address the question of simultaneous measurability or unmeasurability of these quantities [1,7]. Our experimental method of obtaining the uncertainty relation yields results equivalent to that of measuring photon-number variance directly, and on a separate subensemble, measuring phase variance directly. If an attempt is made at simultaneous (i.e., joint) measurement of two canonically conjugate variables on an individual ensemble member, then the result would be an uncertainty product which is larger than the above method. This result is connected to the requirement that the simultaneous measurement of two canonically conjugate observables necessarily adds additional noise [8,9].

Before discussing in detail number-phase uncertainty relations, one must clarify how the phase variable is to be defined. The problem of defining the phase of an electromagnetic field has generated much recent interest, and several different phase definitions have been proposed. One method of defining the phase is to define operators (Hermitian or operational) which correspond to the phase or to the sine and cosine of the phase [10–15]. Another definition is the Wigner phase distribution, which is a marginal Wigner distribution [16]. In this paper, we measure phase distributions corresponding to the Pegg-Barnett Hermitian phase operator and to the Wigner marginal distribution. In the case of a Hermitian phase operator $\hat{\phi}$, it is easy to formulate the uncertainty relation [Eq. (1)]. In the case of the Wigner phase distribution, there is no corresponding Hermitian phase operator. In fact, for some states the Wigner phase distribution can be negative, which implies that it is not a true phase distribution but a quasidistribution [17]. Thus there is no device which can directly measure the Wigner phase on individual trials. There is no obvious way to define a physi-

cally meaningful number-phase uncertainty principle using the Wigner phase definition. It is also possible to formulate number-phase uncertainty relations in terms of a probability operator measure (POM), which is related to a set of complete operators which are not necessarily Hermitian. Shapiro and Shepard have devised a POM for the phase of the field [18]. They show that the results obtained using the POM are equivalent to those obtained using Hermitian operators proposed by Susskind and Glogower [10] and by Pegg and Barnett [11,12].

We will concentrate on the Pegg-Barnett phase operator in this paper. We choose to do this because of the conceptual simplicity of Hermitian operators—it is possible to apply familiar quantum mechanical principles. As stated above, the results obtained using this operator can also be obtained using the POM of Shapiro and Shepard, but the interpretations of the uncertainty relation using the two methods are different.

Previous experiments have measured a quantity called the “dispersion” D [19] of the optical phase for weak coherent-state signals [13–15,20–22]. The dispersion squared is defined as

$$D^2 = \langle \Delta \cos^2 \phi \rangle + \langle \Delta \sin^2 \phi \rangle, \quad (2)$$

where $\langle \Delta \cos^2 \phi \rangle = \langle \cos^2 \phi \rangle - \langle \cos \phi \rangle^2$. In the limit of the well-defined phase, the dispersion squared is approximately equal to the phase variance $\Delta \phi^2 = \langle \phi^2 \rangle - \langle \phi \rangle^2$, while for a uniform phase distribution the dispersion is 1 and the variance is $\pi^2/3$ [19]. In these previous experiments, the reason that the dispersion was measured instead of the variance is because the operators being considered were sine and cosine operators for the field. Since our experiments determine the phase distribution, we will work with the phase variance [4,5,23].

We know of no way to directly test the uncertainty relation [Eq. (1)] for the Pegg-Barnett phase operator (or the Shapiro-Shepard POM). This is because we know of no way to directly measure the phase operator (or the POM). Even if a direct measurement scheme for the Pegg-Barnett phase operator could be found, direct measurement of the commutator would be impossible, since in this case it is non-Hermitian. The only known way to determine all of the quantities in the number-phase uncertainty relation is via our state measurement technique.

In the case of the measured coherent states, which are found to be pure, our method yields an experimentally determined complex wave function for the field mode.

In Sec. II we examine the method of state determination via OHT recently developed by us. It is shown that the measurement of the Wigner function can be achieved by measuring many distributions of quadrature amplitude in many different representations and then inverting this data via tomography. Section III describes the experimental measurement technique. Here we present results for the Wigner function, the density matrix (and since the states we measure are pure, the wave function), and the

photon-number variance. The Pegg-Barnett and Wigner definitions of phase are described in Sec. IV. The measured probability distributions for both definitions of phase are presented here and compared to theory. In Sec. V we examine the uncertainty relation for number and phase of a single-mode coherent state. The experimental results are shown and compared with the theory based on the Pegg-Barnett formalism. It is seen that the experimental results agree quite well with the theory.

II. STATE DETERMINATION

Our measurements are based on determining the quantum-mechanical state of a field mode. The method we use to do this is called optical homodyne tomography. This technique is discussed in greater detail elsewhere [4,5], and only a brief review will be given here.

Quadrature operators for the electric field are defined as $\hat{x} = (\hat{a} + \hat{a}^\dagger)/\sqrt{2}$ and $\hat{p} = (\hat{a} - \hat{a}^\dagger)/i\sqrt{2}$, where \hat{a} is the annihilation operator for a particular spatial-temporal mode of the field. The operators \hat{x} and \hat{p} correspond to the real and imaginary parts of the electric field, respectively. From these operators, rotated quadrature operators can be defined as $\hat{x}_\theta = \hat{x} \cos \theta + \hat{p} \sin \theta$ and $\hat{p}_\theta = -\hat{x} \sin \theta + \hat{p} \cos \theta$. In terms of these operators, the electric-field operator is

$$\begin{aligned} \hat{E}(t) &= E_0(t) [\hat{x} \cos(\omega t) + \hat{p} \sin(\omega t)] \\ &= E_0(t) [\hat{x}_\theta \cos(\omega t + \theta) + \hat{p}_\theta \sin(\omega t + \theta)], \end{aligned} \quad (3)$$

where ω is the optical frequency and $E_0(t)$ corresponds roughly to the electric-field strength of a pulse containing a single photon. A balanced homodyne detector makes measurements which correspond to the quadrature operator \hat{x}_θ of the signal field, when the local-oscillator field is in a large-amplitude coherent state [24,25]. The spatial-temporal mode of the signal field which is selected by the homodyne detector is the same as that of the local oscillator, and the measured quadrature is determined by the phase of the local oscillator θ .

In our experiments, an ensemble of measurements of quadrature amplitudes x_θ are made to determine the probability distributions $P_\theta(x_\theta)$ for various values of θ . These distributions can be written in terms of the Wigner function $W(x, p)$ of the field mode as

$$P_\theta(x_\theta) = \int_{-\infty}^{\infty} W(x_\theta \cos \theta - p_\theta \sin \theta, x_\theta \sin \theta + p_\theta \cos \theta) dp_\theta. \quad (4)$$

For a set of such probability distributions determined on a continuous set of angles θ , it was shown by Vogel and Risken that the distributions could be inverted using the inverse radon transformation to obtain the Wigner function [3]:

$$W(x, p) = \frac{1}{4\pi^2} \int_{-\infty}^{\infty} dx_\theta \int_{-\infty}^{\infty} d\xi |\xi| \int_0^\pi d\theta P_\theta(x_\theta) \exp[i\xi(x_\theta - x \cos \theta - p \sin \theta)]. \quad (5)$$

If distributions are available for a finite, discrete, set of angles between 0 and π , the inversion of Eq. (5) can still be performed using numerical techniques familiar in tomographic imaging [26,27]. The resulting reconstruction of the Wigner function is unique as long as the measured probability distributions are completely contained within a finite range of x_θ . If $W(x,p)$ does not have structure on a scale finer than the sampling scale, the reconstruction accurately reproduces $W(x,p)$. The dynamic range and resolution of our measurement apparatus ensures that our measured probability distributions satisfy these requirements for the coherent states described here.

From the measured Wigner function, it is possible to construct the density matrix of the measured field mode by numerically performing a one-dimensional Fourier transform [28]

$$\langle x+x'|\hat{\rho}|x-x'\rangle = \int_{-\infty}^{\infty} W(x,p)e^{2ipx'} dp. \quad (6)$$

Since the density matrix completely determines the quantum-mechanical state of a system, optical homodyne tomography provides a way to determine this state. The density matrix of Eq. (6) is expressed in the x representation; it will be useful later to have the density matrix in the representation of the number states $|n\rangle$. This change of basis is accomplished by computing overlap integrals of the density matrix in the x representation with Hermite polynomials:

$$\begin{aligned} \langle n|\hat{\rho}|m\rangle &= \left[\frac{1}{\pi 2^n 2^m n! m!} \right]^{1/2} \\ &\times \int_{-\infty}^{\infty} dx \int_{-\infty}^{\infty} dx' e^{-(1/2)(x^2+x'^2)} H_n(x) \\ &\times H_m(x') \langle x|\hat{\rho}|x'\rangle. \quad (7) \end{aligned}$$

In our experiment the signal field was prepared in coherent states of differing average photon number. These states were used for two reasons: first, they are easy to produce and measure, and second, the theory for the uncertainty relation is relatively easy to work out and compare to the experiments. The Wigner function of a coherent state $|\alpha\rangle$ is given by

$$W(x,p) = \frac{1}{\pi} e^{-[(x-\bar{x})^2 + (p-\bar{p})^2]}, \quad (8)$$

where \bar{x} and \bar{p} are the mean values of x and p [i.e., $\bar{x} = (\alpha + \alpha^*)/\sqrt{2}$ and $\bar{p} = (\alpha - \alpha^*)/i\sqrt{2}$]. Thus the Wigner function is a two-dimensional Gaussian function, centered about the point (\bar{x}, \bar{p}) , with standard deviations of $\sqrt{2}$ in the x and p directions. The mean number of photons in the coherent state described by Eq. (8) is $\bar{n} = \frac{1}{2}(\bar{x}^2 + \bar{p}^2)$.

When performing the numerical inversion to obtain the Wigner function, we use the standard filtered back projection algorithm for parallel-beam sampling geometry [26,27]. Using the directly measured distributions $P_\theta(x_\theta)$, the Wigner function reconstruction occurs on a grid in the (x,p) plane that is centered about the origin. This is fine for fields which have zero mean, for which the Wigner function is contained in a region centered about the origin (such as squeezed-vacuum states [4,5]). For

fields with nonzero mean, we have found that the numerical inversion is much more efficient and accurate if the reconstruction window is shifted so that its center at (x',p') corresponds approximately to the center of the reconstructed Wigner function. This is accomplished by numerically shifting the measured probability densities according to $P_\theta(x_\theta) \rightarrow P_\theta(x_\theta - x' \cos\theta - p' \sin\theta)$. It can be seen from Eq. (5) that the effect of reconstructing these shifted distributions is to shift the center of the Wigner function according to $W(x,p) \rightarrow W(x-x', p-p')$. The window over which the measured Wigner function is reconstructed is then centered about the point (x',p') . The widths of the reconstruction window in the x and p directions are taken to be approximately eight times the standard deviation of the probability distributions $P_\theta(x_\theta)$, which ensures that all of the structure in the Wigner function is obtained. Outside the reconstruction window, the measured Wigner function is zero.

III. EXPERIMENTAL MEASUREMENTS

The experimental layout is shown in Fig. 1. The mode-locked, Q -switched, cavity-dumped Nd:YAG laser (where YAG denotes yttrium aluminum garnet) produces 300-ps, nearly transform-limited pulses at 1064 nm with a repetition rate of 420 Hz and a pulse-energy stability of $\pm 3\%$. The pulses are split with a polarizing beam splitter (PBS1) to create the signal and local oscillator (LO) beams; these two beams form two arms of a Mach-Zehnder interferometer. Half-wave plates and neutral density filters in each arm of the interferometer are used to control the relative intensities of these two beams. The piezoelectric translator pushes a mirror which adjusts the phase of the local oscillator. Each LO pulse contains approximately 2×10^6 photons, while the number of photons in the signal pulse is varied between zero and about 10. The signal and LO pulses, which are orthogonally polarized, are superimposed both temporally and spatially on a polarizing beam splitter (PBS2) with nominally

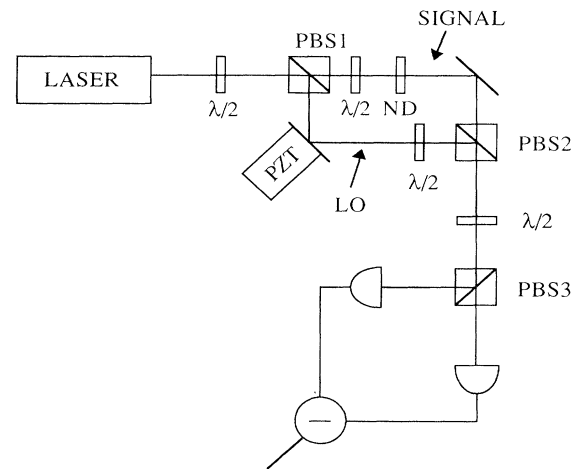


FIG. 1. The experimental apparatus. In this figure, PBS denotes a polarizing beam splitter, $\lambda/2$ denotes a half-wave plate, PZT denotes a piezoelectric translator, and ND represents a neutral-density filter.

zero time delay. Our balanced homodyne detector consists of a $\lambda/2$ plate, a polarizing beam splitter (PBS3) and high-quantum-efficiency ($\eta \sim 85\%$) In-Ga-As photodiodes. The combination of the $\lambda/2$ plate, which rotates the polarizations of the signal and local oscillator fields by 45° , and a polarizing beam splitter (PBS3) serves to interfere the signal and local oscillator fields and to act as a 50/50 beam splitter whose two output fields are detected by the photodiodes. The photodiode outputs are electronically subtracted and integrated using a low-noise charge-sensitive preamplifier [29]. For each laser pulse, this subtracted and integrated signal yields the photoelectron difference number between the outputs of the two detectors. This balancing arrangement removes most of the additive classical noise on the LO and allows us to make measurements at the shot-noise level (SNL) [30]. The electronic noise variance is approximately six times lower than the local-oscillator SNL, which is defined as the variance of photoelectron counts from a coherent-state LO.

A. Wigner function

We have measured Wigner functions for coherent-state signal fields with several different mean numbers of photons, with one of these shown in Fig. 2. For each field strength, we make 5000 repeated measurements of the photoelectron difference number N_θ at 11 values of the local oscillator phase equally spaced in a $[0, \pi]$ interval and calculate photoelectron distributions $P_{N_\theta}(N_\theta)$. Since the signal beam is in a coherent state and the number of photons in the signal beam is much smaller than the number in the local oscillator beam, the variance of each of these photoelectron distributions yields the SNL of the LO, denoted by $\bar{N}_{LO,\theta}$, for a data set with a given value of θ . By averaging the variances of the distributions for different θ , the SNL \bar{n}_{LO} is determined. The difference number is scaled to yield the quadrature amplitude using $x_\theta = N_\theta / (2\bar{n}_{LO})^{1/2}$. Thus the $P_{N_\theta}(N_\theta)$ distributions can be scaled to yield distributions $P_\theta(x_\theta)$ of the quadrature

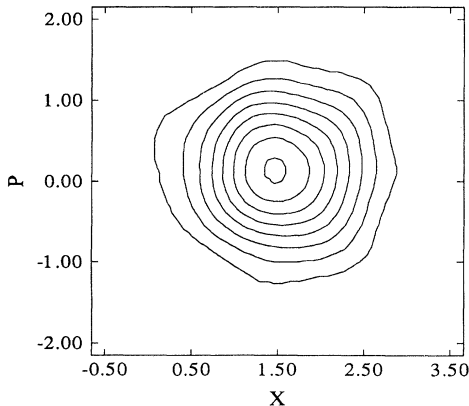


FIG. 2. The measured Wigner function of a coherent state containing an average number of photons of 1.2. The equal-amplitude contours are separated by increments of 0.04.

amplitudes. From these distributions we use the inverse radon transform to calculate the Wigner function, as described above. The LO SNL, \bar{n}_{LO} , can be determined in an independent manner by blocking the signal beam and one detector and directly measuring the number of LO photoelectrons which hit the other detector. Since the detectors are balanced, the total number of LO photoelectrons is twice this measured number. These two methods of obtaining the scaling factor $(\bar{n}_{LO})^{1/2}$ agree to within 4% [29].

B. Density matrix and wave function

Optical homodyne tomography determines the density matrix for arbitrary states, be they mixed or pure. In our experiments, we anticipate the signal to be in a pure coherent state. A sufficient condition that a density matrix describe a pure state is $\text{Tr}(\hat{\rho}^2) = 1$. When these traces are calculated for our experimentally determined density matrices, they are found to equal 1.00 ± 0.02 . The measured fields are thus pure states to a high degree. Since there is no reason to expect our measured states to be nonclassical (i.e., having a nonpositive definite Glauber-Sudarshan P distribution), and the only classical states that are pure states are coherent states [31], this indicates that our measured states must be well described by coherent states. This is not surprising, despite the fact that there are losses in our system. The purity of nonclassical states is destroyed by losses, but a coherent state that has suffered loss is still a coherent state, it just has a smaller amplitude [32]. The $\pm 3\%$ energy fluctuations from our laser do not destroy the purity of these weak coherent states. It is easily shown that the total noise on a classical signal field is

$$\Delta n^2 = \bar{n} + \Delta E^2, \quad (9)$$

where \bar{n} is the shot noise and ΔE^2 is the classical noise due to pulse energy fluctuations (normalized to photon number units) [33]. For fields with a fixed $\pm 3\%$ classical noise, as the field becomes weaker ΔE^2 becomes smaller more rapidly than \bar{n} . For fields with $\bar{n} \lesssim 50$ and classical energy fluctuations of $\pm 3\%$, the shot noise dominates and the classical noise has little effect on the field statistics (e.g., with $\bar{n} = 50$ and $\pm 3\%$ classical fluctuation, $\Delta E^2 \cong 9$).

If the state determined by OHT is found to be pure, it is possible to express the measured density matrix as a wave function. In terms of the density matrix in the x -quadrature representation, the wave function in this representation is

$$\psi(x) = |\psi(x)\rangle e^{i[B(x) + \beta_0]} = \frac{\langle x | \hat{\rho} | 0 \rangle}{\sqrt{\langle 0 | \hat{\rho} | 0 \rangle}} e^{i\beta_0}, \quad (10)$$

where $\beta(x)$ is the complex phase of the wave function and β_0 is an arbitrary constant phase. A similar equation exists for the wave function in the p -quadrature representation $\tilde{\psi}(p)$. Since the coherent states that we have measured have been found to be pure to a high degree, it is thus possible to construct wave functions for these states.

Shown in Fig. 3 is the wave function of a measured

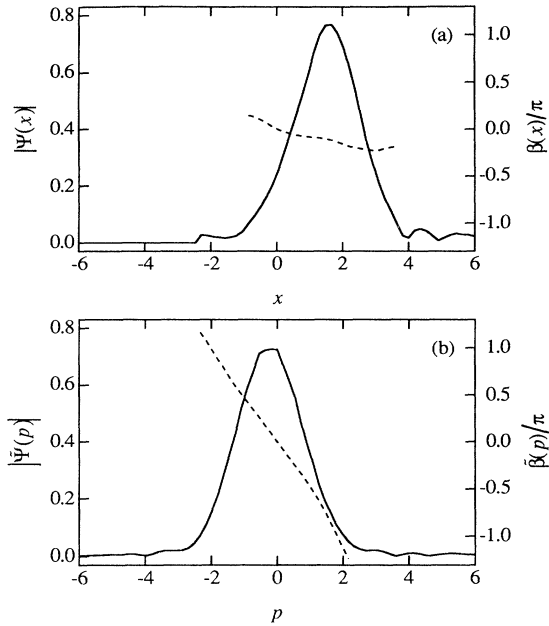


FIG. 3. The measured wave function of a coherent state containing an average of 1.2 photons in (a) the x -quadrature representation and (b) the p -quadrature representation. The solid line is the magnitude $|\Psi|$ of the wave function and is plotted against the left axis, while the dashed line is the phase β of the wave function, plotted against the right axis.

coherent state with a mean number of photons of 1.2. The wave function is plotted in both the x and p representations. The wave function squared $|\psi(x)|^2 [|\tilde{\psi}(p)|^2]$ is the probability density for observing the real [imaginary] part of the electric field with a particular value. It is seen that in the x representation, the wave function is offset from zero and has a phase that is approximately constant. The p -representation wave function is centered at zero and has a phase that is linear in p . The linear dependence of the phase $\beta(x)$ on x [and $\beta(p)$ on p] implies that the field is in a coherent state. The wave functions in the two representations have these properties because of the Fourier transform relationship that exists between them.

C. Photon number

Information about the photon number in the signal beam can be obtained in several ways. The photon-number distribution $P(n)$ can be obtained by directly integrating the Wigner function with Laguerre polynomial weight functions [34]. Alternatively, the density matrix in the number-state representation [Eq. (6)] can be used to obtain the photon-number distribution $\langle n | \hat{\rho} | n \rangle$ [5,23]. These two methods are found to yield the same photon-number distributions to within the precision of the procedure. The precision is estimated by examining the $P(n)$ distribution for large values of n . For signal fields with finite numbers of photons, $P(n)$ should approach zero for large n . We find that $P(n)$ decreases to a level of approximately 0.005 at large n and then fluctuates randomly between ± 0.005 . We thus estimate our accuracy

in determining $P(n)$ to be approximately ± 0.005 . Shown in Fig. 4 are measured photon-number distributions for coherent states with average photon numbers of 0.2, 1.2, and 3.6.

When calculating moments of the signal photon number, we find that it is best not to use the photon-number distributions obtained from the above-described methods. The reason for this is that the distributions do not decay completely to zero and they must thus be truncated at some point; hence the moments are sensitive to exactly where the distribution is truncated. The higher the moment, the more sensitive it is to the truncation. To avoid this problem, when calculating moments of the photon number, the photon-number operator $\hat{n} = \hat{a}^\dagger \hat{a}$ is written in terms of the quadrature operators $\hat{n} = \frac{1}{2}(\hat{x}^2 + \hat{p}^2 - 1)$. The quadrature operators are then placed in Weyl order and the moments can be calculated as c -number integrals of the measured Wigner function [28]. For example, the moment $\langle \hat{n}^2 \rangle$ can be calculated using

$$\begin{aligned} \langle \hat{n}^2 \rangle &= \frac{1}{4} \langle [\hat{x}^4 + \hat{p}^4 + \hat{x}^2 \hat{p}^2 + \hat{p}^2 \hat{x}^2 - 2\hat{x}^2 - 2\hat{p}^2 + 1] \rangle \\ &= \frac{1}{4} \langle [\hat{x}^4 + \hat{p}^4 + 2\hat{x}^2 \hat{p}^2 - 2\hat{x}^2 - 2\hat{p}^2]_{\text{Weyl}} \rangle \\ &= \frac{1}{4} \int_{-\infty}^{\infty} \int_{-\infty}^{\infty} dx dp (x^4 + p^4 + 2x^2 p^2 \\ &\quad - 2x^2 - 2p^2) W(x, p). \end{aligned} \quad (11)$$

We estimate that the determination of the mean number of photons in the detected mode using this technique is accurate to better than 8%, limited by drift and noise of the LO pulses and of the electronics, as well as the finite number of $P_\theta(x_\theta)$ distributions. The mean number of photons calculated from the measured Wigner distribution can be compared to the directly measured number

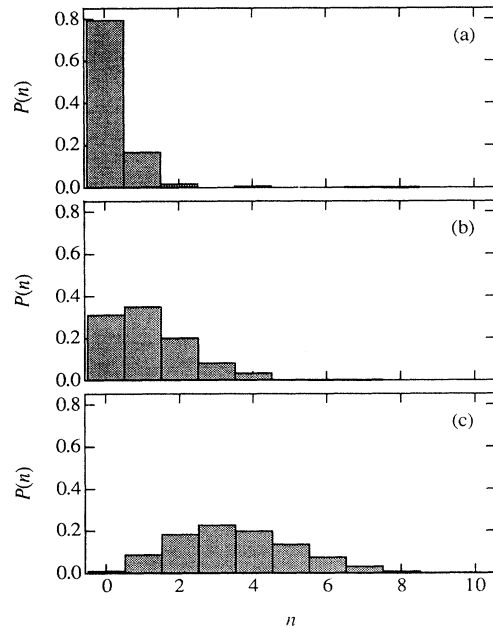


FIG. 4. Photon-number distributions for measured coherent states containing on average (a) 0.2, (b) 1.2, and (c) 3.6 photons.

of photons in the signal beam. We cannot measure the 0.1–10 photons present in the signal beam, but we can directly measure the signal beam when it contains on the order of 10 000 photons, and then attenuate this signal with calibrated neutral density filters. This direct measurement is only accurate to within a factor of 2 because of the accuracy of the filter calibration and the error in measuring the number of photons present. The number of photons calculated from the Wigner distribution is typically smaller than the directly measured number of photons by a factor of 1.7 (e.g., for one particular measurement we obtain a mean of 1.3 photons from the Wigner measurement, while the direct measurement yields two photons).

IV. PHASE

One possible means of describing the phase of a quantum-mechanical field is in terms of the Pegg-Barnett Hermitian phase operator $\hat{\phi}$ [11,12]. This operator is defined in a finite- (but arbitrarily large) dimensional Hilbert space. In an $(s+1)$ -dimensional Hilbert space the phase states are defined as

$$|\phi\rangle = \frac{1}{\sqrt{s+1}} \sum_{n=0}^s e^{in\phi} |n\rangle. \quad (12)$$

This Hilbert space is spanned by a complete orthonormal set of basis phase states $|\phi_m\rangle$, given by Eq. (12) with ϕ replaced by

$$\phi_m = \phi_0 + \frac{2\pi m}{s+1}, \quad m=0, 1, \dots, s, \quad (13)$$

where ϕ_0 is a reference phase. In terms of the states $|\phi_m\rangle$ the Hermitian phase operator is

$$\hat{\phi} = \sum_{m=0}^s \phi_m |\phi_m\rangle \langle \phi_m|. \quad (14)$$

With this definition, the phase states are the eigenstates of the phase operator, i.e., $\hat{\phi}|\phi\rangle = \phi|\phi\rangle$. In our experiments ϕ actually corresponds to the phase difference between the signal and the LO field.

Using the Pegg-Barnett formalism, one can define a probability distribution for the phase. For a signal mode in a state described by a density operator $\hat{\rho}$, the probability of measuring a particular value of the phase is $P_{\text{PB}}(\phi) = [(s+1)/2\pi] \langle \phi | \hat{\rho} | \phi \rangle$, which is normalized so that the integral of $P_{\text{PB}}(\phi)$ over a 2π region of ϕ is equal to 1. In terms of the number-state basis, this distribution is

$$P_{\text{PB}}(\phi) = \frac{1}{2\pi} \sum_{n,m=0}^s e^{i(m-n)\phi} \langle n | \hat{\rho} | m \rangle. \quad (15)$$

For all of the coherent states we have measured ($\bar{n} \leq 8$), the phase distribution described by Eq. (15) converges for $s \geq 20$.

Another way to characterize the phase of a field is via the Wigner phase distribution $P_W(\phi)$ [16]. This is defined as the overlap in phase space of the Wigner distribution and a narrow “wedge-shaped” region,

$$P_W(\phi)\Delta\phi = \int_{\phi}^{\phi+\Delta\phi} d\phi' \int_0^{\infty} dr r W(r \cos\phi', r \sin\phi'). \quad (16)$$

For a coherent state, using Eqs. (8) and (16), we find that the Wigner phase distribution is given by

$$P_{W,\text{CS}}(\phi) = \frac{e^{-2\bar{n}}}{2\pi} \left\{ 1 + \sqrt{2\pi\bar{n}} e^{2\bar{n} \cos^2\phi} \times \cos\phi [1 + \text{erf}(\sqrt{2\bar{n}} \cos\phi)] \right\}, \quad (17)$$

where $\text{erf}(\)$ denotes the error function and the limit $\Delta\phi \rightarrow 0$ has been taken.

Using Eqs. (15) and (16) it is straightforward to calculate the phase distributions for our experimentally measured states. In Fig. 5(a) we compare the measured Wigner and Pegg-Barnett phase distributions for coherent states with different amplitudes. It is seen that as the mean photon number decreases, the phase distribution broadens, as would be expected from the uncertainty principle. It is also seen that the Wigner phase distribution is more peaked than the Pegg-Barnett, as is expected from previous theoretical results [35] and experiments on squeezed states [5,23]. Shown in Fig. 5(b) are the theoretical phase distributions for coherent states with the same mean photon number as in Fig. 5(a). The theoretical results are obtained from Eqs. (15) and (17).

Once the phase distributions are computed, moments of the phase can easily be calculated using these distributions. Shown in Fig. 6 are the measured variances of the Wigner and Pegg-Barnett phase distributions as a function of the mean number of photons in the signal field. As pointed out above, the variance of the Wigner phase distribution is smaller than the corresponding variance for the Pegg-Barnett distribution. This difference is most pronounced when the coherent state has mean number of

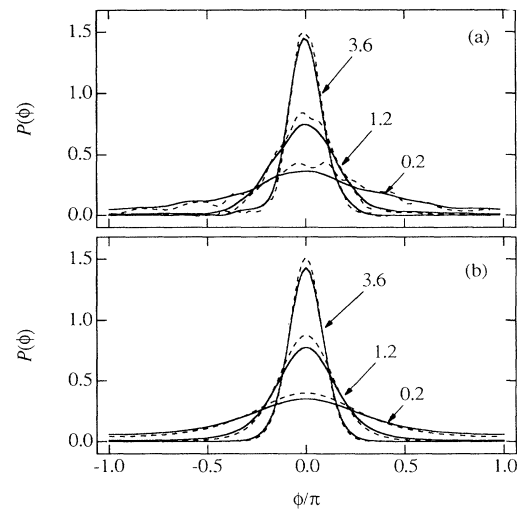


FIG. 5. The solid lines are the Pegg-Barnett and the dashed lines are the Wigner phase distributions for (a) measured and (b) theoretical coherent states. The mean number of photons for the states is indicated.

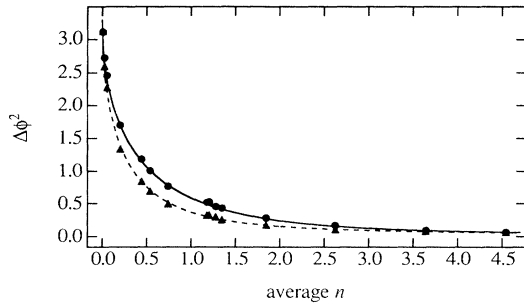


FIG. 6. The variance of the phase is plotted against the average number of photons in a coherent state. The points are experimentally determined values for the Pegg-Barnett (circles) and Wigner (triangles) phase definitions. The curves are the theoretical values for the Pegg-Barnett (solid line) and Wigner (dashed line) phase definitions.

photons approximately equal to 1, while for smaller and larger coherent states the variances are approximately equal for the two distributions. Also plotted in Fig. 6 are the theoretical variances for a coherent-state signal field. Explicit formulas for the phase variance of the Pegg-Barnett phase of a coherent state are given in Ref. [22]. The variance for the Wigner phase is easily calculated numerically using the distribution in Eq. (17). The agreement between the experimental data and the theory is seen to be quite good and again indicates that the states we are measuring in the experiment are well described by coherent states.

V. UNCERTAINTY PRINCIPLE

The uncertainty relation for the phase $\hat{\phi}$ and photon number \hat{n} operators is given by the standard form of Eq. (1) [1]. In terms of number states, the commutator can be written [11]

$$[\hat{\phi}, \hat{n}] = \frac{2\pi}{s+1} \times \sum_{n=0}^s \sum_{\substack{n'=0 \\ n' \neq n}}^s |n'\rangle \langle n| \frac{(n-n') \exp[i(n'-n)\phi_0]}{\exp[i(n-n')2\pi/(s+1)] - 1}. \quad (18)$$

Since this is an operator, its expectation value for the state of interest must be determined to set the lower bound of experimental measurements of $\Delta\phi\Delta n$ [36].

Note that the state dependence of the number-phase uncertainty relation is in contrast to the uncertainty relation for the field quadrature amplitudes (analogous to the position and momentum of a harmonic oscillator, i.e., $\Delta x \Delta p \geq 1/2$, which is independent of the state). The uncertainty relation for the quadrature field amplitudes when the field is in a squeezed state was experimentally verified by Wu, Xiao, and Kimble, who compared the measured uncertainty product of the quadrature amplitudes to the theoretical lower bound [37]. For pure squeezed, or coherent, states of the field, the uncertainty relation for the quadrature operators achieves an equality $\Delta x \Delta p = \frac{1}{2}$.

Plotted in Fig. 7 are both the uncertainty product $\Delta\phi\Delta n$ and the expectation value of the commutator $\frac{1}{2}|\langle[\hat{\phi}, \hat{n}]\rangle|$ for our experimentally measured data. For the experimental data, the commutator expectation value is calculated numerically by expressing the matrices for $\hat{\phi}$ and \hat{n} in the number-state representation, evaluating the matrix which corresponds to the commutator, and tracing the commutator over the density matrix in the number-state representation. Also plotted are the theoretically predicted values for coherent states. For the theoretical uncertainty product, $\Delta\phi$ was calculated in the same fashion as used to generate Fig. 6, while the photon-number standard deviation was calculated using $\Delta n = \sqrt{\bar{n}}$ for a coherent state. Notice that the uncertainty relation is satisfied (as it must be using our method of analysis); the uncertainty product is greater than the expectation value of the commutator. It is interesting, however, that the equality between these two quantities is only achieved for average photon numbers approaching zero or approaching a very large number. This is true for both the theoretical and experimental data, so it is not simply a manifestation of our measurements. This means that, despite their purity, coherent states are not “intelligent” states with respect to number and phase. Intelligent states are defined as states for which Eq. (1) is an equality [6]. Of course, the only coherent state which is a minimum-uncertainty state is the vacuum, for which $\Delta\phi\Delta n = 0$. It is seen that in the limit of very small or very large coherent-state amplitude, the coherent states are approximately number-phase intelligent.

It is interesting to speculate as to the origin of the coherent state’s nonintelligent property. Coherent states are eigenstates of the annihilation operator, which is closely related to the quadrature operators, and these states are intelligent relative to these variables, i.e., $\Delta x \Delta p = \frac{1}{2}|\langle\psi|[\hat{x}, \hat{p}]|\psi\rangle| = \frac{1}{2}$. On the other hand, coherent states are not closely related to the phase eigenstates [11,12]. Therefore, there is no reason to expect them to be number-phase intelligent. In contrast, both number states and phase eigenstates are number-phase intelligent [6].

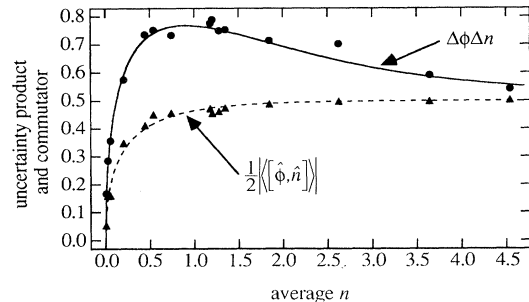


FIG. 7. The number-phase uncertainty product and expectation value of the number-phase commutator are plotted against the average number of photons in a coherent state. The points are experimentally determined values for the uncertainty product (circles) and the commutator expectation (triangles). The curves are the theoretical values for the uncertainty product (solid line) and the commutator expectation (dashed line).

VI. CONCLUSIONS

We have developed a technique for experimentally determining the standard deviation of the phase $\Delta\phi$ and photon number Δn , as well as the expectation value of their commutator $|\langle[\hat{\phi}, \hat{n}]\rangle|$, for a mode of an optical field. Although we have concentrated on the results for coherent-state signal fields, nowhere in the measurements was it necessary to assume that the field was in a coherent state [38]. This method of field characterization will in principle work for *arbitrary* states of the field—the only limitation being the available experimental parameters (i.e., detector efficiency, resolution, etc.). It is thus possible to experimentally measure, for any state of the field, how close to uncertainty relation [Eq. (1)] comes to equality (provided, of course, that the field can be identically prepared many times so that an ensemble of measurements can be made to determine its Wigner function).

These results were possible because optical homodyne tomography determines the quantum-mechanical state (as described by a density matrix) of a mode of the field. Since the measured states were found to be relatively pure, it was possible to determine the complex wave functions corresponding to these states.

The agreement between the measured and theoretical points in Figs. 6 and 7 is ensured by the agreement between the measured and theoretical density matrices. Therefore, other phase definitions could be used, also leading to good agreement of experiment and theory. For this reason our results do not favor one phase definition over another.

Our measurements naturally yield the Wigner function of the field mode. Given $W(x,p)$ one can also construct the Q distribution by convolving $W(x,p)$ with a vacuum-state Wigner function [39]. The marginal Q phase distribution can then be constructed in analogy with Eq. (16) [40]. The resulting phase variance is larger than that from the marginal Wigner phase distribution shown in Fig. 6. This Q phase distribution corresponds to that which would be obtained using the eight-port homodyne apparatus of Walker and Carroll [41] and of Noh, Fougères, and Mandel [13–15] (see also [39,42–44]). The increase in the width of this distribution can be associated with additional noise introduced when measuring both x and p quadratures simultaneously. A rigorous uncertainty relation for the simultaneous (but imprecise) measurement of n and ϕ , which is possible using this apparatus, would have to be developed with this particular experimental arrangement in mind. The result for the uncertainty product $\Delta\phi\Delta n$ for simultaneous number and phase measurements would necessarily be larger than the product $\Delta\phi\Delta n$ that we determined and show in Fig. 7.

ACKNOWLEDGMENTS

We wish to acknowledge several helpful discussions with H. Carmichael, G. Milburn, and W. Schleich. We thank A. Faridani for providing us with the software for performing the inverse Radon transform. This research is supported by the National Science Foundation, Grant No. PHY 8921709-01.

*Permanent address: Joint Institute for Laboratory Astrophysics and the Department of Physics, University of Colorado and the National Institute of Standards and Technology, Boulder, CO 80309.

- [1] L. I. Schiff, *Quantum Mechanics*, 3rd ed. (McGraw-Hill, New York, 1968).
- [2] M. Beck, D. T. Smithey, J. Cooper, and M. G. Raymer, *Opt. Lett.* **18**, 1259 (1993).
- [3] K. Vogel and H. Risken, *Phys. Rev. A* **40**, 2847 (1989).
- [4] D. T. Smithey, M. Beck, A. Faridani, and M. G. Raymer, *Phys. Rev. Lett.* **70**, 1244 (1993).
- [5] D. T. Smithey, M. Beck, J. Cooper, M. G. Raymer, and A. Faridani, *Phys. Scr.* (to be published).
- [6] J. A. Vaccaro and D. T. Pegg, *J. Mod. Opt.* **37**, 17 (1990).
- [7] V. B. Braginsky and F. Y. Khalili, *Quantum Measurement* (Cambridge University Press, Cambridge, 1992).
- [8] E. Aurthurs and J. L. Kelley, Jr., *Bell Syst. Tech. J.* **44**, 725 (1965).
- [9] Y. Yamamoto and H. A. Haus, *Rev. Mod. Phys.* **58**, 1001 (1986).
- [10] L. Susskind and J. Glogower, *Physics* **1**, 49 (1964).
- [11] D. T. Pegg and S. M. Barnett, *Phys. Rev. A* **39**, 1665 (1989).
- [12] S. M. Barnett and D. T. Pegg, *J. Mod. Opt.* **36**, 7 (1989).
- [13] J. W. Noh, A. Fougères, and L. Mandel, *Phys. Rev. Lett.* **67**, 1426 (1991).
- [14] J. W. Noh, A. Fougères, and L. Mandel, *Phys. Rev. A* **45**, 424 (1992).
- [15] J. W. Noh, A. Fougères, and L. Mandel, *Phys. Rev. A* **46**, 2840 (1992).
- [16] W. Schleich, R. J. Horowicz, and S. Varro, *Phys. Rev. A* **40**, 7405 (1989).
- [17] B. M. Garraway and P. L. Knight, *Phys. Rev. A* **46**, R5346 (1992).
- [18] J. H. Shapiro and S. R. Shepard, *Phys. Rev. A* **43**, 3795 (1991).
- [19] Z. Hradil, *Quantum Opt.* **4**, 93 (1992).
- [20] H. Gerhardt, U. Büchler, and G. Litfin, *Phys. Lett.* **49A**, 119 (1974).
- [21] M. M. Nieto, *Phys. Lett.* **60A**, 401 (1977).
- [22] R. Lynch, *Phys. Rev. A* **41**, 2841 (1990).
- [23] M. Beck, D. T. Smithey, and M. G. Raymer, *Phys. Rev. A* **48**, R890 (1993).
- [24] H. P. Yuen and J. H. Shapiro, *IEEE Trans. Inf. Theory* **IT-26**, 78 (1980).
- [25] W. Vogel and W. Schleich, *Phys. Rev. A* **44**, 7642 (1991).
- [26] F. Natterer, *The Mathematics of Computerized Tomography* (Wiley, New York, 1986).
- [27] A. Faridani, *Inverse Problems and Imaging; Pitman Research Notes in Mathematics*, edited by G. F. Roach (Wiley, Essex, 1991), Vol. 245, p. 68.
- [28] M. Hillery, R. F. O'Connell, M. O. Scully, and E. P. Wigner, *Phys. Rep.* **106**, 121 (1984).
- [29] D. T. Smithey, M. Beck, M. Belsley, and M. G. Raymer, *Phys. Rev. Lett.* **69**, 2650 (1992).
- [30] H. P. Yuen and V. W. S. Chan, *Opt. Lett.* **8**, 177 (1983).

- [31] M. Hillery, *Phys. Lett.* **111A**, 409 (1985).
- [32] Z. Y. Ou, C. K. Hong, and L. Mandel, *Opt. Commun.* **63**, 118 (1987).
- [33] R. Loudon, *The Quantum Theory of Light*, 2nd ed. (Clarendon, Oxford, 1983).
- [34] T. Marshall and E. Santos, *J. Mod. Opt.* **38**, 1463 (1991).
- [35] G. S. Agarwal, S. Chaturvedi, K. Tara, and V. Srinivasan, *Phys. Rev. A* **45**, 4904 (1992).
- [36] If the phase is defined in terms of the POM of Ref. [18], then the uncertainty relation is defined in terms of a Fourier transform pair, and it is not necessary to measure the commutator.
- [37] L. A. Wu, M. Xiao, and H. J. Kimble, *J. Opt. Soc. Am. B* **4**, 1465 (1987).
- [38] The scaling of the photon-counting distributions to obtain the quadrature distributions as described here relied on the fact that the field was in a coherent state. It is possible to properly scale the distributions without any assumption as to the state of the field, as was done in Refs. [4] and [5].
- [39] Y. Lai and H. A. Haus, *Quantum Opt.* **1**, 99 (1989).
- [40] W. Schleich, A. Bandilla, and H. Paul, *Phys. Rev. A* **45**, 6652 (1992).
- [41] N. G. Walker and J. E. Carroll, *Opt. Quantum Electron.* **18**, 355 (1986).
- [42] M. Freyberger and W. Schleich, *Phys. Rev. A* **47**, R30 (1993).
- [43] M. Freyberger, K. Vogel, and W. Schleich (private communication).
- [44] The original experiment of Ref. [41] did not make measurements at the shot-noise level, so phase distributions from this experiment would not be true quantum phase distributions. To obtain the Q phase distribution using the technique described in Refs. [13–15], it is necessary for one of the two input beams to be in a large amplitude coherent state [39,42,43].